Broadly wavelength- and pulse width-tunable high-repetition rate light pulses from soliton self-frequency shifting photonic crystal fiber integrated with a frequency doubling crystal

Aleksandr A. Lanin,[1] Andrei B. Fedotov,[1] and Aleksei M. Zheltikov[1,2,*]

[1]*Physics Department, International Laser Center, M.V. Lomonosov Moscow State University, Moscow 119992, Russia*

[2]*Department of Physics and Astronomy, Texas A&M University, College Station, Texas 77843-4242, USA*

**Corresponding author: zheltikov@physics.tamu.edu*

Received June 4, 2012; revised July 15, 2012; accepted July 15, 2012;
posted July 16, 2012 (Doc. ID 169852); published August 27, 2012

Soliton self-frequency shift (SSFS) in a photonic crystal fiber (PCF) pumped by a long-cavity mode-locked Cr:forsterite laser is integrated with second harmonic generation (SHG) in a nonlinear crystal to generate ultrashort light pulses tunable within the range of wavelengths from 680 to 1800 nm at a repetition rate of 20 MHz. The pulse width of the second harmonic output is tuned from 70 to 600 fs by varying the thickness of the nonlinear crystal, beam-focusing geometry, and the wavelength of the soliton PCF output. Wavelength-tunable pulses generated through a combination of SSFS and SHG are ideally suited for coherent Raman microspectroscopy at high repetition rates, as verified by experiments on synthetic diamond and polystyrene films.

OCIS codes: 190.5530, 190.7110.

Following the demonstration of unique properties and excellent performance of photonic crystal fibers (PCFs) as frequency converters and supercontinuum sources [1–3], waveguides of this class find growing applications as components of larger-scale laser systems and optical devices for a broad variety of applications, including frequency comb metrology [4], attosecond science [5], and optical parametric amplification of few-cycle field waveforms [6]. In optical imaging, PCFs have been advantageously integrated into the apparatus for coherent Raman microscopy [7,8], radically simplifying the design of a multicolor optical source required for this method of imaging. PCF-based probes combined with the protocols of optogenetics [9] offer much promise for the development of advanced optical interfaces for neuroscience [10]. The integration of PCF supercontinuum sources with frequency conversion in nonlinear crystals has been shown to allow the generation of ultrashort pulses within a broad spectral range from the UV to the near-IR [11], as well as to enable the creation of ultracompact sources of terahertz pulses [12].

Here, we demonstrate that soliton self-frequency shift (SSFS) in a PCF pumped by an increased energy output of a long-cavity mode-locked Cr:forsterite laser can be combined with second harmonic generation (SHG) in a nonlinear crystal to provide a broad wavelength and pulse width tunability of ultrashort light pulses in the range of wavelengths from 680 to 1800 nm at 20 MHz repetition rate. This yields ultrashort light pulses with an average power up to 10 mW ideally suited for coherent Raman microspectroscopy.

In experiments, we employ a homebuilt ytterbium-fiber-laser-pumped mode-locked Cr:forsterite laser oscillator [13], which delivers laser pulses with a central wavelength of 1.25 μm [the dashed line in Fig. 1(a)] and a pulse width of 40 to 70 fs. The extended cavity design of the Cr:forsterite laser allows the output laser energy to be increased up to 18 nJ at a pulse repetition rate of 20 MHz. The Cr:forsterite laser output is launched into a silica PCF with parameters as specified in [17] [inset to Fig. 1(a)]. This PCF was designed to provide efficient wavelength conversion of 1.25 μm laser pulses through SSFS, delivering tunable ultrashort light pulses within a wavelength range of 1.35 to 1.80 μm. The core diameter of the PCF was chosen large enough (4 μm) to allow an increase in the energy of solitons [13] relative to the typical level of soliton energies attainable with highly nonlinear PCFs.

The spectrum of the soliton output of a 20 cm long PCF pumped by 5 nJ, 68 fs Cr:forsterite [Fig. 1(a)] features an isolated wavelength-shifted soliton centered at 1550 nm (35% incoupling loss and 25% pump-to-soliton energy conversion efficiency) with a bandwidth supporting a transform-limited pulse width of 47 fs. Wavelength tunability of the soliton PCF output is illustrated by Fig. 1(b), which presents the spectra of frequency-shifted solitons generated in a 20 cm section of PCF by Cr:forsterite laser pulses with different energies.

The wavelength-shifted PCF output was frequency doubled through SHG in an xz-cut LBO crystal. Frequency doubling of short-pulse fiber-laser output has been earlier shown to provide a compact wavelength-tunable source of subpicosecond pulses [14]. Our experiments demonstrate that the wavelength tunability range can be further expanded and broad pulse width tunability can be added by combining PCF-based SSFS with SHG in a properly optimized nonlinear crystal. For each wavelength from the tunability range provided by SSFS in the PCF used in our experiments [Fig. 1(b)], the angle ϕ of the wave vector of the pump field with respect to the y axis in the xy plane [see the inset in Fig. 2(a)] was chosen in such a way as to provide phase matching for $o + o \rightarrow e$ SHG at the desired [the dashed line in Fig. 2(b)]. The spectra of the second harmonic produced by the wavelength-shifted solitons from the PCF in 2 and 20 mm LBO crystals are presented in Figs. 2(a) and 2(b), respectively. In the range of input

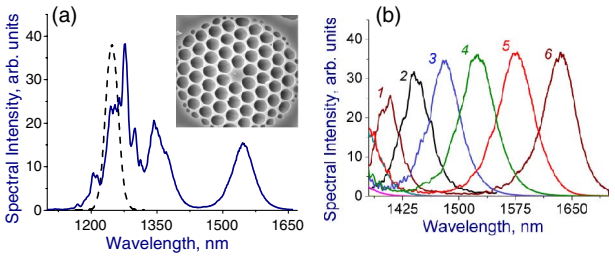

Fig. 1. (Color online) (a) Spectrum of Cr:forsterite laser pulses (dashed line) and spectrum at the output of a 20 cm piece of PCF (shown in the inset) measured with an input energy of 5 nJ (solid line); (b) spectra of wavelength-shifted solitons at the output of a 20 cm piece of PCF measured with an input energy of 3.5 nJ (1), 4 nJ (2), 4.4 nJ (3), 4.9 nJ (4), 6.3 nJ (5), and 7.5 nJ (6).

wavelengths from 1400 to 1500 nm, the 20 mm LBO crystal provided a typical SHG efficiency of about 40%, yielding second harmonic pulses in the 690 to760 nm wavelength range with an energy up to 0.5 nJ. Thus, in the case of a long nonlinear crystal, the spectral brightness of the second harmonic in our experiments was higher than the spectral brightness of the soliton, which becomes possible, as demonstrated in the earlier work [14], due to $(\omega_0 + \delta) + (\omega_0 - \delta) = 2\omega_0$ sum-frequency generation processes. The average output peak power of no less than 10 mW was achieved within the entire range from 690 to 750 nm. Beyond this region, the output power gradually decreased, reaching ~5 mW at 860 nm. A thinner, 2 mm LBO crystal provided the second harmonic output power above 4.0 mW within the range from 680 to 760 nm, decreasing to 1.8 mW at 860 nm. Ultrashort pulses in this wavelength range, albeit with much lower energies, can be generated directly by using ultrasmall core tapered fibers [15].

The pulse width of the second harmonic generated in the LBO crystal can be tuned by varying the thickness of the nonlinear crystal, beam-focusing geometry, and the wavelength of the soliton PCF output, providing the pump field for the SHG process. Due to the mismatch of the group velocities u_p and u_{SH} of the pump and second harmonic pulses in an SHG crystal, the pulse width of the second harmonic increases [16] in accordance with $\tau_{SH} \approx (\tau_p^2/2 + \theta^2)^{1/2}$, where τ_p is the pulse width of the pump, $\theta = l_{int}(u_p^{-1} - u_{SH}^{-1})$, $l_{int} = \min(L, b)$ is the interaction length, L is the thickness of the nonlinear crystal, $b = 2\pi w_0^2/\lambda_0$ is the confocal parameter, λ_0 is the pump wavelength, and w_0 is the waist radius of the pump beam. The second harmonic pulse width calculated as a function of the pump and second harmonic wavelengths for a thin ($L = 2$ mm) and a thick ($L = 20$ mm) nonlinear crystals is shown by the dashed lines in Fig. 3(a). Dispersion of the nonlinear crystal was included in these calculations through the Sellmeier equation with appropriate coefficients for LBO. In the case of a thin nonlinear crystal, a lens with a focal length $f = 7.5$ cm is used, giving $b = 3.8$ mm for $\lambda_0 = 1500$ nm. In this regime, $L < b$ and τ_p is close to θ, giving rise to a weak dependence of τ_{SH} on λ_0 [curve 1 in Fig. 3(a)]. In the case of a thick crystal, we take $f = 15$ cm, leading to $b = 13.5$ mm for $\lambda_0 = 1500$ nm. In this case, $\tau_p \ll \theta$ and $\tau_{SH} \approx b(u_p^{-1} - u_{SH}^{-1})$, leading to a strong dependence of τ_{SH} on λ_0 controlled by the dispersion of the nonlinear crystal [curve 2 in Fig. 3(a)].

Typical autocorrelation traces of second harmonic pulses produced with thin (2 mm) and thick (20 mm) BBO crystals are presented in Fig. 3(b). These traces were measured using the SHG process in a 0.5 mm thick BBO crystal. The second harmonic output of a 2 mm LBO crystal centered at 700 nm [curve 1 in Fig. 3(b)] can be accurately fitted with a Gaussian envelope with an FWHM pulse width of 73 fs. For the 20 mm crystal, the pulse width of second harmonic output ranged from 210 to 600 fs within the range of wavelengths from 700 to 800 nm. A typical autocorrelation trace for the second harmonic at 790 nm is shown by curve 2 in Fig. 3(b), corresponding to an FWHM pulse width of 580 fs. The pulse width of the second harmonic output measured as a function of λ_0 for 2 mm and 20 mm thick nonlinear crystals is shown by the circles and rectangles, respectively, in Fig. 3(a). Results of these experiments agree well with theoretical predictions [dashed lines in Fig. 3(a)],

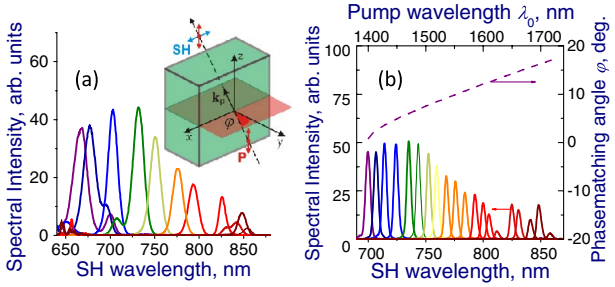

Fig. 2. (Color online) Spectra of the second-harmonic output of (a) a 2 mm and (b) 20 mm thick LBO crystal pumped by wavelength-shifted solitons from a 20 cm long PCF. The dashed line in (b) shows the SHG phase-matching angle ϕ as a function of the soliton pump (the upper abscissa axis) and the second harmonic (the lower abscissa axis) wavelength for LBO. Diagram of the $o + o \rightarrow e$ SHG process in an xz-cut LBO crystal is shown in the inset: P, pump field; SH, second harmonic; and ϕ, angle between the wave vector of the pump beam and the y axis in the xy plane.

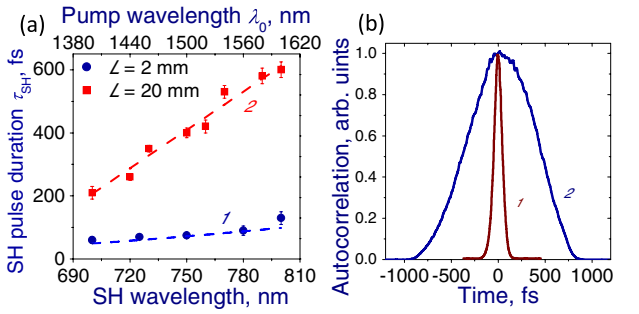

Fig. 3. (Color online) (a) Pulse width of the second harmonic as a function of the pump (upper abscissa axis) and second harmonic (lower abscissa axis) wavelengths: results of experiments using an LBO crystal with $L = 2$ mm (circles) and 20 mm (rectangles) versus calculations for $L = 2$ mm (dashed curve 1) and 20 mm (dashed curve 2); (b) autocorrelation traces of (1) the 700 nm and (2) 790 nm second harmonic output of (1) a 2 mm and (2) 20 mm thick LBO crystal pumped by wavelength-shifted solitons from a 20 cm long PCF.

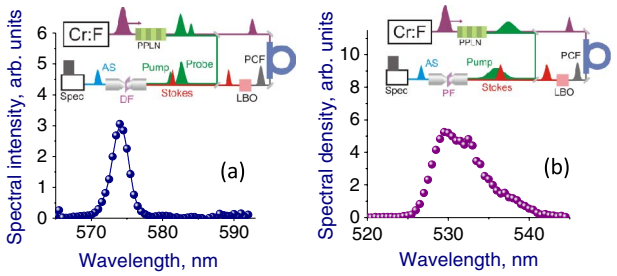

Fig. 4. (Color online) CARS spectra of the 1332 cm^{-1} zone-center $\Gamma^{(25+)}$ (F_{2g}) symmetry optical phonon in a synthetic diamond film. (a) The 2850 cm^{-1} CH vibrational mode of polystyrene and (b) experimental (dots) and theoretical (solid lines) fits assuming Lorentzian line profiles for the Raman lines. Diagrams of CARS arrangement are shown in the insets: Cr:F, Cr:forsterite laser; PPLN, periodically poled lithium niobate waveguide; PCF, photonic crystal fiber; DF, diamond film; PF, polymer film; AS, anti-Stokes signal; and Spec, spectrometer.

showing that the second harmonic pulse width can be varied from 70 to 600 fs.

Simultaneous wavelength and pulse width tunability provided by a combination of the SSFS and SHG technologies is especially helpful for nonlinear Raman spectroscopy and microscopy, where the wavelength tunability is needed for a selective excitation of Raman modes, while the pulse width tunability is instrumental in reducing the coherent background [17], related to nonresonant four-wave mixing, in the overall coherent Raman response. In Figs. 4(a) and 4(b), we present typical spectra of coherent anti-Stokes Raman scattering (CARS) obtained for synthetic diamond and polystyrene films. The pump field at a fixed wavelength, $\lambda_p \approx 623$ nm, was delivered by the Cr:forsterite laser output frequency doubled in a periodically poled lithium niobate (PPLN) waveguide [the inset in Fig. 4(a)], providing 15 to 20 mW of laser power on the sample. The Stokes field with a tunable wavelength λ_s was delivered by PCF-based SSFS combined with SHG as described above. In experiments with synthetic diamond, the 1332 cm^{-1} zone-center $\Gamma^{(25+)}$ (F_{2g}) symmetry optical phonon [18] was excited through the Raman process by tuning the Stokes wavelength to $\lambda_s \approx 680$ nm. Coherently driven optical phonon vibrations in diamond were read out with a probe pulse [the inset in Fig. 4(a)], also provided by the second harmonic output of the PPLN waveguide, giving rise to an anti-Stokes signal centered at $\lambda_a \approx 575$ nm [Fig. 4(a)]. The total acquisition time required to record the full spectrum of this signal was 4 to 5 s. The probe pulse was applied with a delay time of 400 fs relative to the pump and Stokes pulses in order to reduce the coherent background in the overall signal [19]. In the case of polystyrene, the Stokes wavelength was tuned to $\lambda_s \approx 758$ nm in order to excite the CH vibrational mode at 2850 cm^{-1}. The probe pulse was applied simultaneously with the pump and Stokes pulses [the inset in Fig. 4(b)], giving rise to an anti-Stokes signal at $\lambda_a \approx 529$ nm observed against an intense coherent background due to the nonresonant four-wave mixing process [Fig. 4(b)].

In conclusion, soliton self-frequency shift in a PCF pumped by a long-cavity mode-locked Cr:forsterite laser has been integrated with SHG in a nonlinear crystal to generate 20 MHz repetition rate ultrashort light pulses wavelength-tunable from 680 to 1800 nm, thus expanding the wavelength-tunability range well beyond tunability attainable with the same class of commercially available systems. In addition to wavelength-tunability, the technology demonstrated in this work offers broad pulse width tunability, yielding ~10 mW optical field waveforms with pulse widths tunable from 70 to 600 fs ideally suited for coherent Raman microspectroscopy.

Valuable assistance by A. P. Ovvyan in pulse duration measurements is gratefully acknowledged. This work was partially supported by the Seventh European Framework Programme (CROSS TRAP 244068) and Russian Foundation for Basic Research.

References

1. P. St. J. Russell, Science **299**, 358 (2003).
2. J. M. Dudley, G. Genty, and S. Coen, Rev. Mod. Phys. **78**, 1135 (2006).
3. A. M. Zheltikov, Phys. Uspekhi **47**, 69 (2004).
4. Th. Udem, R. Holzwarth, and T. W. Hänsch, Nature **416**, 233 (2002).
5. P. B. Corkum and F. Krausz, Nat. Phys. **3**, 381 (2007).
6. C. Y. Teisset, N. Ishii, T. Fuji, T. Metzger, S. Köhler, R. Holzwarth, A. Baltuška, A. M. Zheltikov, and F. Krausz, Opt. Express **13**, 6550 (2005).
7. E. R. Andresen, V. Birkedal, J. Thøgersen, and S. R. Keiding, Opt. Lett. **31**, 1328 (2006).
8. D. A. Sidorov-Biryukov, E. E. Serebryannikov, and A. M. Zheltikov, Opt. Lett. **31**, 2323 (2006).
9. K. Deisseroth, Nat. Methods **8**, 26 (2011).
10. L. V. Doronina, I. V. Fedotov, A. A. Voronin, O. I. Ivashkina, M. A. Zots, K. V. Anokhin, E. Rostova, A. B. Fedotov, and A. M. Zheltikov, Opt. Lett. **34**, 3373 (2009).
11. H. Liu, M. Hu, B. Liu, Y. Song, L. Chai, A. M. Zheltikov, and C. Wang, J. Opt. Soc. Am. B **27**, 2284 (2010).
12. F. Liu, Y. Song, Q. Xing, M. Hu, Y. Li, C. Wang, L. Chai, W. Zhang, A. M. Zheltikov, and C. Wang, IEEE Photon. Technol. Lett. **22**, 814 (2010).
13. A. B. Fedotov, A. A. Voronin, I. V. Fedotov, A. A. Ivanov, and A. M. Zheltikov, Opt. Lett. **34**, 851 (2009).
14. K. Moutzouris, F. Adler, F. Sotier, D. Träutlein, and A. Leitenstorfer, Opt. Lett. **31**, 1148 (2006).
15. T. A. Birks, W. J. Wadsworth, and P. St. J. Russell, Opt. Lett. **25**, 1415 (2000).
16. S. A. Akhmanov, A. P. Sukhorukov, and A. S. Chirkin, J. Exp. Theor. Phys. **28**, 748 (1969).
17. M. Marangoni, A. Gambetta, C. Manzoni, V. Kumar, R. Ramponi, and G. Cerullo, Opt. Lett. **34**, 3262 (2009).
18. M. D. Levenson, C. Flytzanis, and N. Bloembergen, Phys. Rev. B **6**, 3962 (1972).
19. A. A. Lanin, A. B. Fedotov, and A. M. Zheltikov, Opt. Lett. **37**, 1508 (2012).